Simulating the sea level imprint on marine oxygen isotope records during the middle Miocene using an ice sheet–climate model

P. M. Langebroek,[1,2] A. Paul,[1,3] and M. Schulz[1,3]

Received 18 October 2008; revised 8 February 2010; accepted 17 May 2010; published 16 October 2010.

[1] Oxygen isotopic ratios are implemented in an ice sheet–climate model in order to directly compare the modeled isotopic ratio of the seawater to the high-resolution isotopic records from deep-sea sediment cores in the middle Miocene. The isotopic depletion resulting from the modeled ice sheet expansion explains the mean oxygen isotope step found in deep-sea sedimentary records of ~0.5‰. Approximately 85% of the modeled increase in the isotopic composition of seawater is caused by an increase in ice volume; the remainder is due to a stronger depletion in oxygen isotopes in the large ice sheet. Furthermore, we also investigated the relation between sea level (or global ice volume) and the isotopic composition of seawater. Our experiments confirm the validity of the relation of approximately 1‰ enrichment per 100 m sea level lowering. We further show that this relationship is restricted by the mean ocean depth and the assumed oxygen isotopic composition of the ice sheet. Small deviations (±10%) from this general relationship occur depending on the size and the mean isotopic content of the ice sheet. Large continental ice sheets are more depleted in heavy oxygen isotopes and therefore reach a slightly higher ratio. In contrast, small ice sheets have a less depleted isotopic composition and correspondingly have a smaller effect on the isotopic composition of the ocean.

Citation: Langebroek, P. M., A. Paul, and M. Schulz (2010), Simulating the sea level imprint on marine oxygen isotope records during the middle Miocene using an ice sheet–climate model, *Paleoceanography*, *25*, PA4203, doi:10.1029/2008PA001704.

1. Introduction

[2] The ratio of oxygen isotopes measured in the shells of (benthic) foraminifera ($\delta^{18}O_c$, the relative deviation in ‰ from a known external standard) is one of the most commonly used proxies in paleoclimate reconstructions. Interpretation of this ratio is, however, not straightforward, because it is influenced by temperature and the isotopic composition of the water surrounding the foraminifera [*Shackleton*, 1974]. The oxygen isotope ratio of seawater ($\delta^{18}O_{sw}$, deviations with respect to Vienna Standard Mean Ocean Water [*Gonfiantini*, 1978]) itself depends on the global ice volume (V_{ice}), the isotopic composition of the ice ($\delta^{18}O_{ice}$) and local variations [e.g., *Waelbroeck et al.*, 2002]. By stacking deep-sea records from different locations [*Zachos et al.*, 2001; *Lisiecki and Raymo*, 2005] the local $\delta^{18}O_{sw}$ and temperature effects are thought to be reduced and $\delta^{18}O_c$ can be used as a proxy for global ocean temperatures and ice volume. Often, the $\delta^{18}O_c$ record is disentangled using independent temperature proxies (e.g., Mg/Ca [e.g., *Lear et al.*, 2000]). After correcting for the temperature effect, the global ice volume can be approximated assuming a constant $\delta^{18}O_{ice}$ in time.

[3] During the middle Miocene (~13.9 Ma), an increase in benthic $\delta^{18}O_c$ [*Zachos et al.*, 2001; *Holbourn et al.*, 2005] in combination with a global sea level fall [*Miller et al.*, 1998, 2005] strongly indicate a shift toward colder climatic conditions. However, it is still not clear to what extent the increase in $\delta^{18}O_c$ is caused by the expansion of the Antarctic ice sheet, possibly in combination with a change in $\delta^{18}O_{ice}$, and which part is due to a decrease in deep-sea temperature. Low-resolution studies using the ratio of Mg/Ca in benthic foraminifera to separate the temperature from the ice volume effect suggested that the major part (70–85%) of the increase in benthic $\delta^{18}O_c$ during the middle Miocene can be explained by the expansion of continental ice [e.g., *Lear et al.*, 2000; *Shevenell et al.*, 2008].

[4] In this study we used a different approach, focusing on the ice sheet part of the proxy (following the work of *Mix and Ruddiman* [1984], *Lhomme et al.* [2005] and *Sima et al.* [2006]). In our ice sheet–climate model, fluctuations in Antarctic ice volume as well as variations in $\delta^{18}O_{ice}$ were computed. Resulting $\delta^{18}O_{sw}$ anomalies could then directly be compared to the deep-sea records of benthic oxygen isotopes. We applied this technique to the large-scale cooling event in the middle Miocene and found that indeed a significant part of the deep-sea record can be explained by Antarctic glaciation. The direct effect of the continental ice buildup accounted for the major part of the transition. Only approximately 15% is caused by a shift in mean isotopic content of the ice sheet.

[1]Faculty of Geosciences, University of Bremen, Bremen, Germany.
[2]Now at Alfred Wegener Institute for Polar and Marine Research, Bremerhaven, Germany.
[3]MARUM–Center for Marine Environmental Sciences, University of Bremen, Bremen, Germany.

0883-8305/10/2008PA001704

[5] Combining ice volume and $\delta^{18}O_{ice}$ (or $\delta^{18}O_{sw}$) in a coupled model also creates a unique opportunity to investigate the relation between these parameters. Previous estimates range from 0.8–2.2‰ increase in $\delta^{18}O_c$ per 100 m sea level fall [*Fairbanks and Matthews*, 1978; *Schrag et al.*, 1996; *Pekar et al.*, 2002]. We tested this relationship and show that a 1‰ increase in the isotopic composition of seawater is related to a sea level lowering of approximately 100 m, if the mean isotopic composition of the ice sheet is fixed at around −35‰. Including the effect of changes in mean $\delta^{18}O_{ice}$ caused deviations from the relationship of approximately 10%.

2. Methods and Experimental Setup

2.1. Ice Sheet–Climate Model

[6] The coupled ice sheet–climate model is an extension of the ice sheet model used by *Sima et al.* [2006]. It has been adapted to Antarctica and is described in detail by *Langebroek et al.* [2009]. In the version used in this research, the oxygen isotope ratio of ice ($\delta^{18}O_{ice}$) is implemented as a passive tracer (as for the Laurentide ice sheet in the work of *Sima et al.* [2006]). The coupled ice sheet–climate model consists of three large-scale boxes spanning the entire southern hemisphere and is symmetric around the axis of the South Pole. Energy is conserved and redistributed by meridional energy transport, taking into account the latent heat fluxes due to evaporation and snow accumulation. In the two lower-latitude boxes (0–30°S and 30–60°S) climatic parameters (e.g., temperature, T; albedo, α) are described as mean values for the entire box, representing mainly atmospheric processes. Although oceanic processes are not included, seasonally varying sea ice (and its albedo) is computed, following the near-surface air temperatures. Parameters in the high-latitude box (60–90°S) are resolved at a higher resolution of 0.5° latitude.

[7] This Antarctic high-latitude box includes separate atmospheric and surface energy balances that are solved simultaneously and that are influenced by atmospheric heat transport from the surrounding large-scale boxes. The mass balance of the Antarctic ice sheet within this box depends on the daily accumulated precipitation, evaporation and ablation, possibly reduced by (surface and/or bottom) melting and calving. Snowfall is parameterized and depends on the distance to the South Pole (r), surface height (h_{sfc}) and daily surface temperature (T_s) [*Oerlemans*, 2002, 2004]:

$$A = (c_a + c_b r) e^{\frac{-h_{sfc}(r)}{c_d}} e^{\kappa T_s}. \quad (1)$$

[8] This parameterization is tuned to the present-day total accumulation on Antarctica and its latitudinal distribution. In equation (1), c_a and c_b are set to 4.44×10^{-4} m day^{-1} and 1.96×10^{-9} day^{-1}, c_d is a characteristic length scale (3000 m) and κ a constant describing the precipitation dependence on temperature (0.0345 K^{-1}) [see also *Langebroek et al.*, 2009]. Bottom melting occurs if temperature in the bottom layer exceeds the pressure melting point. At the rim of the ice sheet calving occurs if the ice becomes too heavy (thick) to float. The total mass balance is then set to a negative value [*Pollard*, 1982].

[9] The entire model is forced by daily insolation (depending on orbital parameters [*Berger*, 1978a, 1978b; *Laskar et al.*, 2004]) combined with prescribed atmospheric partial pressure CO_2 (pCO_2).

[10] Modeled present-day annual mean temperature is 14.9°C for the southern hemisphere, and this value increases by 2.5°C when pCO_2 is doubled from 280 ppm (the preindustrial value) to 560 ppm (well within the range of 2.1 to 4.4°C estimated from atmospheric general circulation models [*Intergovernmental Panel of Climate Change*, 2007; see also *Langebroek et al.*, 2009]).

[11] The initial ice-free bedrock topography is reconstructed using the present-day bedrock elevation and ice thickness from the BEDMAP project database [*Lythe et al.*, 2000], assuming local isostasy. For the axially symmetric ice sheet model (having no explicit longitudinal direction) we constructed a bedrock profile with a bulge near the rim of the Antarctic continent and a flatter hinterland, resembling East Antarctica.

[12] Modeled ice thickness and height in every grid cell are derived by solving the continuity equation [e.g., *Payne and Dongelmans*, 1997] taking into account local bedrock isostasy, surface mass balance and (if occurring) basal melting.

[13] Within the ice sheet, velocities and temperatures are computed in each of the 12 vertical layers following Glen's flow law [e.g., *Glen*, 1955; *Payne and Dongelmans*, 1997]. In the current extended version, the same advection scheme transporting ice temperature is also used to trace $\delta^{18}O_{ice}$ within the layers. The spatial and temporal parameterizations of surface $\delta^{18}O_{ice}$, or rather the oxygen isotope ratio of snow, are described in sections 2.2 and 2.3.

2.2. Present-Day Spatial Distribution of Oxygen Isotopes

[14] The present-day isotopic composition of snow ($\delta^{18}O_{snow}$) depends on geographical characteristics (latitude, λ; surface elevation, h_{sfc}; distance from the open ocean, d_{sea}) and climatic parameters (annual mean surface temperature, T_{sfc} and precipitation, P). *Giovinetto and Zwally* [1997] compiled a large data set containing mean $\delta^{18}O_{snow}$ values combined with corresponding geographical and climatic parameters for over 400 sites on Antarctica. Their linear regression shows an optimum correlation between $\delta^{18}O_{snow}$ and T_{sfc} according to

$$\delta^{18}O_{snow}[‰] = 0.852 \times T_{sfc}[^\circ C] - 6.78, \quad (2)$$

with a coefficient of determination (r^2) of 0.92. Using several (or all) parameters in multivariate or stepwise regression analysis did not improve the correlation between parameterized and observed $\delta^{18}O_{snow}$. The minor effect of the geographical parameters on the $\delta^{18}O_{snow}$ parameterization is mainly due to the fact that T_{sfc} itself already largely depends on these variables. A more recent publication using a database of more than 1000 locations estimated a similar

linear relationship between T_{sfc} and $\delta^{18}O_{snow}$ (r^2 = 0.92 [*Masson-Delmotte et al.*, 2008]):

$$\delta^{18}O_{snow}[‰] = 0.80 \times T_{sfc}[^{\circ}C] - 8.11. \quad (3)$$

2.3. Past Isotopic Distribution

[15] For reconstructing the past isotopic composition of the Antarctic ice sheet the only available data comes from ice core records. These cores only extend back to ~800 ka [*EPICA Community Members*, 2004] and therefore cannot constrain $\delta^{18}O_{ice}$ during the middle Miocene. Borehole paleothermometry indicates that the spatial relationship between $\delta^{18}O_{snow}$ and T_{sfc} can introduce large errors when used for temporal $\delta^{18}O_{snow}$ reconstructions between the present-day and the Last Glacial Maximum (LGM) in central Greenland [e.g., *Cuffey et al.*, 1995]. On the other hand, atmospheric models for Antarctica suggest that the isotopic-temperature slope remained valid for the LGM [e.g., *Delaygue et al.*, 2000; *Jouzel et al.*, 2007]. Past $\delta^{18}O_{snow}$ can therefore be derived from the present-day spatial distribution of $\delta^{18}O_{snow}$, corrected for local changes in surface elevation (Δh_{sfc}) and changes in mean surface temperature of the ice sheet (ΔT_s) [*Cuffey*, 2000; *Lhomme*, 2004; *Lhomme et al.*, 2005]:

$$\delta^{18}O_{snow}(\lambda, t) = \delta^{18}O_{snow}(\lambda) + \alpha_c \Delta T_s(t) + \beta_\delta \Delta h_{sfc}(\lambda, t), \quad (4)$$

where α_c is the isotopic sensitivity to temperature and β_δ the isotopic lapse rate. According to *Lhomme* [2004] and references therein the value of β_δ is taken as −11.2‰/km, while α_c ranges from 0.6 to 0.8‰/°C.

2.4. Computation of the Oxygen Isotopic Composition of Seawater

[16] The modeled bulk $\delta^{18}O_{ice}$ composition of the Antarctic ice sheet was converted into the oxygen isotopic composition of seawater ($\delta^{18}O_{sw}$) by a simple closed-balance computation, assuming a well-mixed ocean with constant average depth (d_0) and surface area (A_0) similar to present day and by setting the initial $\delta^{18}O_{sw}$ to zero [*Sima et al.*, 2006]:

$$\delta^{18}O_{sw} = -\frac{S_i}{d_0 - S_i}\delta^{18}O_{ice}, \quad (5)$$

where S_i is the Antarctic ice volume equivalent sea level, using ρ_{ice} and ρ_{water} as densities of ice and water, respectively:

$$S_i = \frac{\rho_{ice} V_{ice}}{\rho_{water} A_0}.$$

Accordingly, Antarctica is considered to be the only ice sheet influencing $\delta^{18}O_{sw}$ and changes in sea level. For the experiments during the middle Miocene we focused on the transition from a small to a large ice sheet, therefore the initial conditions were not crucial for the final interpretation. Present-day mean values of 3800 m, 3.605 × 10^{14} m^2, 910 kg/m^3 and 1000 kg/m^3 were used for d_0, A_0, ρ_{ice} and ρ_{water}, respectively. Using the simplified $\delta^{18}O$ rather than tracing the actual mass ratios for all oxygen isotopes in the model introduces a negligible conservation error [*Sima*, 2005].

2.5. Experimental Setup

[17] The ice sheet–climate model was forced by varying time-dependent orbital parameters [*Laskar et al.*, 2004] and several scenarios for pCO_2. The present-day spatial distribution of $\delta^{18}O_{snow}$ was deduced under constant pCO_2 conditions of 280 ppm. The model was spun up for 1 million years (Ma), before comparing the modeled present-day conditions to measured $\delta^{18}O_{snow}$. For the middle Miocene four different constant levels of pCO_2 were used as model forcing, preindustrial (280 ppm) and three levels close to the modeled glaciation threshold of ~615 ppm [*Langebroek et al.*, 2009] (590, 640 and 700 ppm), resulting in two large (pCO_2 levels of 280 and 590 ppm) and two small, ephemeral ice sheets (pCO_2 of 640 and 700 ppm). The scenarios were computed over a period from 14.1 to 13.6 Ma after a 200 ka spin-up, during which the corresponding orbital parameters were used [*Laskar et al.*, 2004]. The $\delta^{18}O_{snow}$ parameterizations were tested for all four resulting ice sheets. Both spatial relations between $\delta^{18}O_{snow}$ and T_{sfc} [*Giovinetto and Zwally*, 1997; *Masson-Delmotte et al.*, 2008] were applied using a set of values for the constants in the temporal parameterization of *Lhomme* [2004]. After these sensitivity experiments, the climatic transition in the middle Miocene was modeled using one of the parameterizations and a pCO_2 reduction from 640 to 590 ppm around approximately 13.9 Ma (see *Langebroek et al.* [2009] for more information about the effect of pCO_2 on the ice sheet–climate model).

2.6. Oxygen Isotope Records Spanning the Middle Miocene

[18] Before discussing the $\delta^{18}O$ results computed by our ice sheet–climate model, we would like to give a brief overview of the characteristics of the available records of the oxygen isotope ratio measured on benthic foraminifera ($\delta^{18}O_c$). To our knowledge only three high-resolution records cover the period between 14.5 and 13.2 Ma (Ocean Drilling Program (ODP) Sites 1146 and 1237 [*Holbourn et al.*, 2005, 2007]) and ODP Site 1171 [*Shevenell et al.*, 2004; *Shevenell and Kennett*, 2004].One additional record covers the middle Miocene transition, but unfortunately terminates at approximately 13.7 Ma [*Raffi et al.*, 2006]. Many other, lower-resolution records are combined into the *Zachos et al.* [2001] compilation. Table 1 and Figure 1 summarize the main features of these records for two particular time periods: before the oxygen isotope shift (13.9–14.5 Ma) and after the transition (13.2–13.8 Ma). The mean increase in $\delta^{18}O_c$ per individual record is approximately 0.5‰.

3. Results

3.1. Present-Day Conditions

[19] Ice volume, temperature and snowfall were tuned to mean present-day values. The modeled present-day ice volume is approximately 25 × 10^{15} m^3 and the mean surface temperature at sea level is about −18 °C, similar to other

Table 1. Characteristics of Benthic Foraminiferal Oxygen Isotope Records During the Middle Miocene Before the Oxygen Isotope Shift (13.9–14.5 Ma) and After the Transition (13.2–13.8 Ma)

	Number of Data		Mean $\delta^{18}O_c$ (‰)			
	Before	After	Before	After	Increase (‰)	Reference
Site 1164	167	251	1.20	1.71	0.51	*Holbourn et al.* [2005]
Site 1237	100	158	1.64	2.15	0.51	*Holbourn et al.* [2005]
Site 1171	82	87	1.50	2.03	0.52	*Shevenell and Kennett* [2004]
Leg 154	601	115	1.84	2.33	0.49	*Raffi et al.* [2006]
Compilation	107	250	1.89	2.23	0.34	*Zachos et al.* [2001]

Antarctic modeling studies [e.g., *Huybrechts et al.*, 2000; *Oerlemans*, 2002]. The mean snowfall (~20×10^{11} m^3), as well as its latitudinal distribution (largest snowfall at the rim of the ice sheet and desert-like conditions at the center), is comparable to reconstructions of accumulation on Antarctica [e.g., *Arthern et al.*, 2006; *van de Berg et al.*, 2006].

[20] Figure 2a shows the modeled annual mean present-day $\delta^{18}O_{snow}$ distribution from our ice sheet–climate model using the parameterizations of *Giovinetto and Zwally* [1997] and *Masson-Delmotte et al.* [2008] (see section 2.2). Results are compared to the database of *Masson-Delmotte et al.* [2008] (red dots in Figure 2). Spatial coverage of the data at high latitudes (poleward of 75°S) remains poor. Therefore the present-day isotopic composition of Antarctic snow from a modeling study using an advanced Rayleigh-type isotope distillation model with 40 year European Centre for Medium-Range Weather Forecasts (ECMWF) Re-Analysis (ERA-40) data as meteorological input [*Helsen et al.*, 2007] is additionally shown for comparison. This type of modeling also has its deficits and is known to underestimate the depletion of $\delta^{18}O_{snow}$ values by ~10% at higher elevations (latitudes) [*Helsen et al.*, 2007]. Our ice sheet–climate model computed a latitudinal distribution comparable to the isotope distillation model with a maximum depletion of approximately −45‰ near the South Pole as compared to values below −50‰ [e.g., *Zwally et al.*, 1998]. Interestingly, the annual mean near surface-air temperatures derived from our ice sheet–climate model fell into the range of measured temperatures in the database of *Masson-Delmotte et al.* [2008] and are colder than ERA-40 temperatures (Figure 2b). Colder temperatures should result in more depleted $\delta^{18}O_{snow}$.

[21] The underestimation of $\delta^{18}O_{snow}$ in the ice sheet model left its imprint on the mean $\delta^{18}O$ of the entire ice sheet ($\delta^{18}O_{ice}$). The parameterizations of *Giovinetto and Zwally* [1997] and *Masson-Delmotte et al.* [2008] resulted in mean $\delta^{18}O_{ice}$ values of −43.7 and −42.8‰, respectively. A different numerical model, combining ice dynamics and tracer transport, indicates more depleted present-day values for the East Antarctic ice sheet of −56.5‰ [*Lhomme et al.*, 2005]. As this paper focuses on temporal variations in $\delta^{18}O$ of the entire ice sheet and the mean $\delta^{18}O_{ice}$ changes between ice sheets of different sizes, we consider the above described parameterizations of $\delta^{18}O_{snow}$ in terms of T_{sfc} to be accurate enough.

[22] Figure 3 shows annual mean temperature, velocity and $\delta^{18}O_{ice}$ in the modeled present-day ice sheet. The annual mean temperatures reach maxima just above the pressure-melting point near the bedrock and minima of ~−50°C at the inland surface. Meridional velocities of over 150 m/yr are computed at the rim of Antarctica and close to zero between 80°S and the South Pole. Vertical velocities are very small everywhere, because of the low accumulation of snow. $\delta^{18}O_{ice}$ shows a similar pattern as the meridional velocities. Most depleted values are found in the center and at the bottom of the ice sheet, with present-day minima of ~−46‰. The coastal surface contains much higher values, closer to −30‰.

3.2. Sea Level and Oxygen Isotopic Composition of Seawater

[23] The four different constant pCO_2 levels resulted in four differently sized ice sheets. Large ice sheets occurred

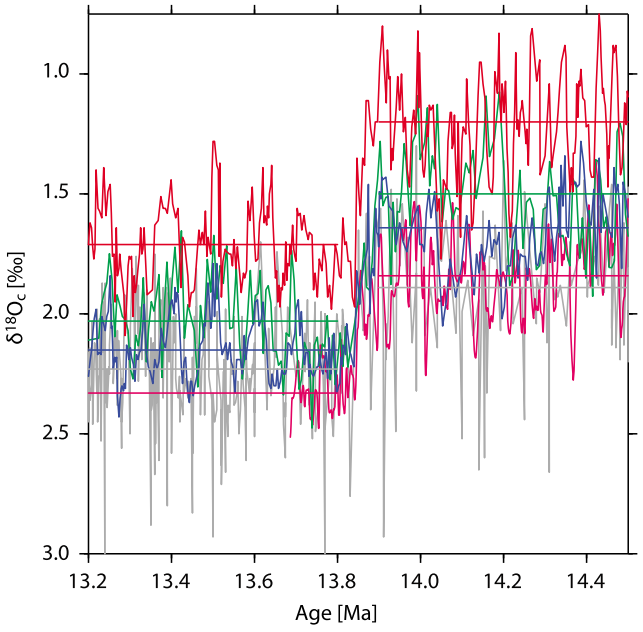

Figure 1. Compilation of high-resolution benthic $^{18}O_c$ records in the middle Miocene. The two records from *Holbourn et al.* [2005] are plotted in blue (Site 1237) and red (Site 1146). Another ODP record (Site 1171), at latitudes closer to Antarctica, is indicated in green-blue [*Shevenell et al.*, 2004] on the same age scale. The record with the highest resolution only extends from ~16.6 Ma to ~13.7 Ma (purple) [*Raffi et al.*, 2006]. The compilation of over 40 records of *Zachos et al.* [2001] is shown in gray for comparison. The mean values for every record in the period before (13.9–14.5 Ma) and after (13.2–13.8 Ma) the transition are indicated by horizontal straight lines (see Table 1).

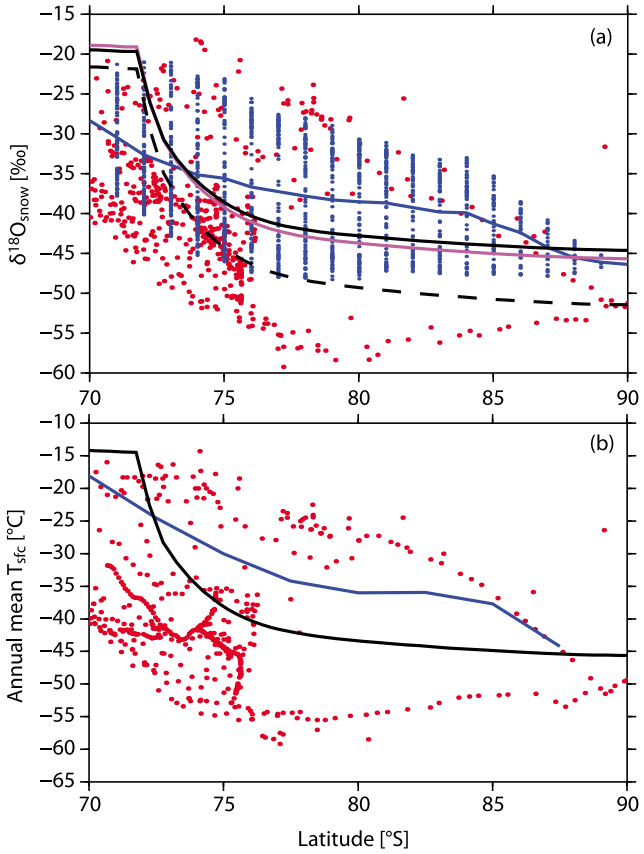

Figure 2. Present-day spatial distribution of (a) $\delta^{18}O_{snow}$ and (b) near-surface air temperature. In Figure 2a, measurements are indicated by red dots (compilation by *Masson-Delmotte et al.* [2008]). The modeled distribution from a Rayleigh-type isotope distillation model forced by ERA-40 data [*Helsen et al.*, 2007] is shown by blue dots; the mean values are connected by the solid blue line. Our model results using $0.852 \times T_{sfc} - 6.78$ [*Giovinetto and Zwally*, 1997] are shown in purple and correspond to a present-day bulk $\delta^{18}O_{ice}$ of −43.1‰. Applying the *Masson-Delmotte et al.* [2008] parameterization ($0.80 \times T_{sfc} - 8.11$) resulted in a mean $\delta^{18}O_{ice}$ values of −42.3‰ (black solid line). The effect of increasing the sensitivity to T_{sfc} in the previous equation to 0.95‰/°C is indicated by the black dashed line. The bulk $\delta^{18}O_{ice}$ then reached −48.7‰. In Figure 2b, temperatures from the reanalysis (ERA-40) and *Masson-Delmotte et al.* [2008] data sets are indicated by blue and red dots, respectively. Results from the ice sheet–climate model from the current study are shown in black.

for 280 and 590 ppm, with mean sizes of 25 and 24×10^{15} m^3, respectively (Table 2). The other two forcings (640 and 700 ppm) generated small ice sheets with mean volumes of 6 and 4×10^{15} m^3. Converted to sea level equivalents, these mean values resulted in approximately 63, 60, 16 and 11 m. The $\delta^{18}O_{ice}$ computed in these experiments was forced by the present-day distribution parameterization of *Masson-Delmotte et al.* [2008] (equation (3)) together with the temporal equation of *Lhomme* [2004] (equation (4); α_c = 0.6‰/°C, β_δ = −11.2‰/km). With decreasing ice volume (increasing pCO_2 forcing), $\delta^{18}O_{sw}$ also decreased (see also Figure 4). Combining all experiments, the relationship between $\delta^{18}O_{sw}$ and sea level showed a slope of approximately 1‰/100 m. Interestingly, this slope reached larger values for large ice sheets and was below this average for small ice sheets. A sea level drop of 100 m would result in a $\delta^{18}O_{sw}$ increase of (0.87 ± 0.02)‰ for small ice sheets and (1.08 ± 0.01)‰ for large ice sheets.

3.3. Sensitivity to $\delta^{18}O_{snow}$ parameterization

[24] To test the robustness of the above described results, we performed a set of sensitivity experiments varying the $\delta^{18}O$ parameterization. In addition to the relationship given by *Masson-Delmotte et al.* [2008] (equation (3)), also the older *Giovinetto and Zwally* [1997] relation (equation (2)) was used as $\delta^{18}O_{snow}$ forcing. For all experiments the parameterization of *Lhomme* [2004] was applied to compute variations in $\delta^{18}O_{snow}$ in the past. Two parameters are used in this approximation: α_c and β_δ. According to *Lhomme* [2004] the former realistically ranges between 0.6 and 0.8‰/°C, whereas the latter is set to −11.2‰/km. Sensitivity analysis for both extremes in α_c were performed, as well as a change of ~10% of the standard value of β_δ (e.g., −10.0 and −12.4‰/km) (Table 3 and Figure 4). The resulting variations in $\delta^{18}O_{sw}$ are quite small. The uncertainty introduced by the $\delta^{18}O_{snow}$ parameterization is less than 5% for $\delta^{18}O_{snow}$ as well as for the estimated $\delta^{18}O_{sw}$–sea level slope.

[25] Regardless of which temporal parameterization of $\delta^{18}O_{snow}$ is used, the $\delta^{18}O_{snow}$ values largely depend on the size (or height) and location of the ice sheet. $\delta^{18}O_{snow}$ becomes more depleted if the ice sheet is larger and/or located further inland.

3.4. Middle Miocene Transition

[26] In *Langebroek et al.* [2009] the ice sheet–climate model is used to constrain the atmospheric CO_2 concentration during the middle Miocene. One of the experiments that shows a good fit to the timing of the glaciation event is forced by a pCO_2 decrease of 640 to 590 ppm, between 13.902 and 13.898 Ma. The same forcing is used in this study in order to create an appropriate transition from a small to a large ice sheet. Before ~13.9 Ma a small ice sheet existed, with a mean ice volume of about 6×10^{15} m^3 or 16 m sea level equivalent (Figure 5). After ~13.9 Ma, when the pCO_2 level dropped to 590 ppm, the Antarctic continent becomes entirely glaciated and the mean ice volume reached 24×10^{15} m^3 (60 m sea level equivalent). During the transition sea level decreased by approximately 44 m. The relationship of 1‰ $\delta^{18}O$ change per 100 m sea level change indicates a marine oxygen isotope increase of 0.44‰ exclusively due to the change in ice volume. However, with the growth of the ice sheet, the bulk $\delta^{18}O_{ice}$ also decreased from ~−31‰ to the more depleted values of a large ice sheet (~−40‰). If the Antarctic ice sheet is the only large continental ice sheet, the development of the small ice sheet would account for an enrichment of the $\delta^{18}O_{sw}$ of mean

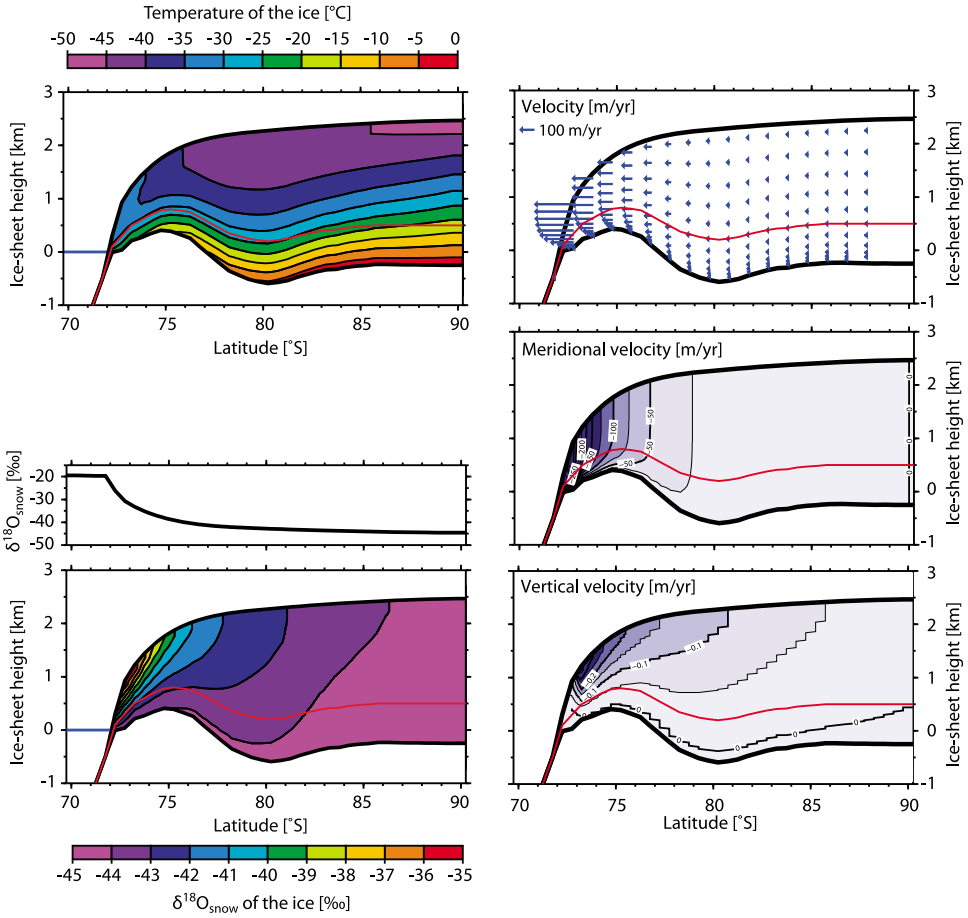

Figure 3. Modeled present-day cross sections through the Antarctic ice sheet. (top left) Temperatures within the ice layers. (bottom left) $\delta^{18}O_{ice}$ with the corresponding distribution of the $\delta^{18}O_{snow}$ on top. (right) Velocity profiles. The thin red line shows the initial bedrock elevation.

ocean water by (0.14 ± 0.01)‰ relative to an ice-free world. The fully grown ice sheet corresponded to a rise of (0.64 ± 0.02)‰, implying a total difference of (0.50 ± 0.02)‰ between a small and a large ice sheet. Figure 6 compares the modeled $\delta^{18}O_{sw}$ curve with two of the high-resolution $\delta^{18}O_c$ records [*Holbourn et al.*, 2005]. The modeled record is shifted such that its mean before the transition corresponds to the mean of the $\delta^{18}O_c$ data prior to large-scale glaciation (13.9–14.5 Ma). The timing as well as the increase in $\delta^{18}O$ in both, the proxy and the modeled, records is very similar. However, the variance in the $\delta^{18}O_{sw}$ data is much smaller than in the measured $\delta^{18}O_c$.

4. Discussion

4.1. Oxygen Isotope Parameterizations

[27] The large present-day data sets of *Giovinetto and Zwally* [1997] and *Masson-Delmotte et al.* [2008] show a high coefficient of determination between $\delta^{18}O_{snow}$ and T_{sfc} of approximately 0.92 for Antarctica. Also the results of the Isotope General Circulation Model Simulations from the SWING (Stable Water Isotope Intercomparison Group) database (http://atoc.colorado.edu/dcn/SWING/index.php) show a very high correlation between $\delta^{18}O_{snow}$ and T_{sfc}. The determination coefficient is around 0.81 for MUGCM and 0.95 for ECHAM4, varying by only a few percent for different model years. The simulations cover a period of 134 a, from 1870 to 2003. Other model experiments show that the Antarctic spatial relationship between $\delta^{18}O_{snow}$ and T_{sfc} remains similar for different time slices over the last 21 ka [*Delaygue et al.*, 2000; *Jouzel et al.*, 2007]. Unfortunately these general circulation models are too time consuming to perform (several) long-term experiments of 500 ka or more.

Table 2. Ice Volume, Sea Level, $\delta^{18}O_{ice}$, $\delta^{18}O_{sw}$, and the Slope Between $\delta^{18}O_{sw}$ and Sea Level for the Four Reference Experiments[a]

	pCO_2 (ppm)			
	280	590	640	700
Ice volume (10^{15} m^3)	25.00	23.73	6.38	4.41
Mean sea level (m)	63.11	59.89	16.11	11.14
Mean $\delta^{18}O_{sw}$ (‰)	0.72	0.64	0.14	0.09
Mean $\delta^{18}O_{ice}$ (‰)	−42.73	−39.75	−31.29	−29.08
Slope ($\delta^{18}O_{sw}$/100 m)	1.08	1.09	0.89	0.85

[a]The $\delta^{18}O$ parameterizations of *Masson-Delmotte et al.* [2008] and *Lhomme* [2004] (with α_c = 0.6‰/°C and β_δ = −11.2‰/km) were applied.

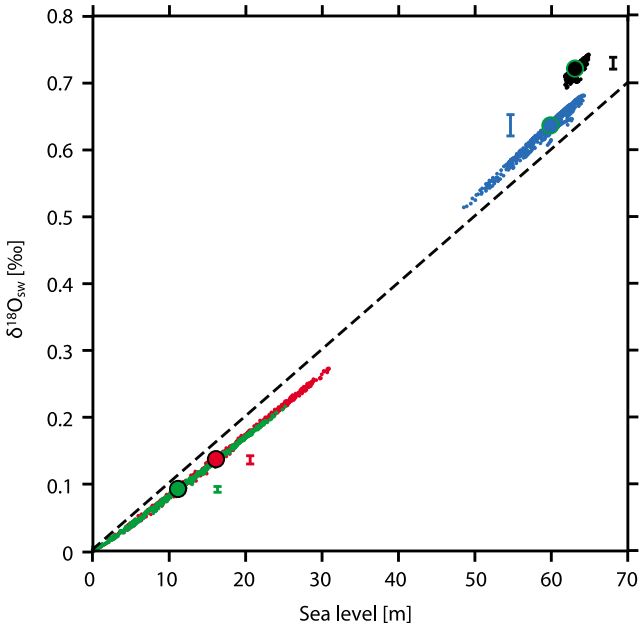

Figure 4. Modeled sea level–$\delta^{18}O_{sw}$ relationship. Shown are reference experiments forced by 280, 590, 640, and 700 ppm (black, blue, red, and green). Here the parameterizations of *Masson-Delmotte et al.* [2008] and *Lhomme* [2004], with α_c = 0.6‰/°C and β_δ = −11.2‰/km, were used. Larger dots indicate the mean of each experiment. The error in $\delta^{18}O_{snow}$ induced by the parameterizations is indicated by the error bars. Dashed line represents the 1‰/100 m relationship.

The strong spatial dependence of $\delta^{18}O_{snow}$ on T_{sfc} could have been less robust in the middle Miocene.

[28] The spatial parameterizations used to describe $\delta^{18}O_{snow}$ resulted in an underestimation of the present-day distribution of $\delta^{18}O$ within the ice sheet (Figure 3). Time-dependent simulations, based on the present-day values of $\delta^{18}O_{snow}$ (corrected for changes in ice sheet elevation and mean temperatures), therefore had too high $\delta^{18}O_{ice}$ values. This could cause problems when the model would be used for specific (ice core) locations (as suggested by *Helsen et al.* [2007]) or for any comparison to events depicted by a specific ice core record. However, the focus of is this study is the relative changes in mean $\delta^{18}O_{ice}$ during the middle Miocene, and the present-day underestimation of $\delta^{18}O_{snow}$ is therefore not crucial.

[29] The temporal parameterization of $\delta^{18}O_{snow}$ derived from observations is valid for a range of values for the constant α_c. We examined the effect of changes in this parameter on the bulk $\delta^{18}O_{ice}$ and computed $\delta^{18}O_{sw}$ by taking the extremes (0.6 and 0.8‰/°C). Higher values resulted in slightly less depleted bulk isotopic compositions of the ice sheet, but the difference in $\delta^{18}O_{sw}$ profiles was vanishingly small (Figure 5). Our sensitivity study implies that the different $\delta^{18}O_{snow}$ parameterization shave only a minor effect (less than 5%) on the computed $\delta^{18}O_{ice}$ (and $\delta^{18}O_{msw}$). Therefore, we applied equation (3) [*Masson-Delmotte et al.*, 2008] and equation (4) [*Lhomme*, 2004], with α_c = 0.6‰/°C and β_δ = −11.2‰/km for the remaining part of this study. If the high spatial correlation between $\delta^{18}O_{snow}$ and T_{sfc} is not valid for the middle Miocene, then also the error in the temporal $\delta^{18}O_{snow}$ parameterizations is larger.

[30] The mean $\delta^{18}O_{ice}$ is not only influenced by the $\delta^{18}O_{snow}$ parameterizations, but also by the amount of snow falling. The snowfall parameterization (equation (1)) is tuned to give a realistic present-day mean value and distribution, and varies with temperature, height and distance from the center of the ice sheet. The relationship between these parameters, as well as the correlation to $\delta^{18}O_{snow}$, could have been different in the past. For example, the open (sub)tropic seaways could have altered the meridional vapor

Table 3. Mean $\delta^{18}O_{sw}$ and $\delta^{18}O_{sw}$–Sea Level (Slope) Results From the Sensitivity Computations[a]

	Temporal (Equation (4))		Mean $\delta^{18}O_{sw}$ (‰)				Slope (‰/100 m)			
Spatial	α_c	β_δ	280	590	640	700	280	590	640	700
Equation (3)	0.6	−11.2	0.722	0.637	0.137	0.093	1.083	1.087	0.886	0.853
Equation (3)	0.8	−11.2	0.722	0.622	0.132	0.089	1.076	1.072	0.858	0.819
Equation (3)	0.6	−12.4	0.721	0.636	0.136	0.092	1.087	1.090	0.877	0.845
Equation (3)	0.8	−12.4	0.722	0.621	0.131	0.088	1.080	1.075	0.848	0.810
Equation (3)	0.6	−10.0	0.722	0.638	0.139	0.094	1.079	1.083	0.895	0.861
Equation (3)	0.8	−10.0	0.723	0.622	0.134	0.090	1.072	1.068	0.867	0.827
Equation (2)	0.6	−11.2	0.738	0.652	0.140	0.095	1.102	1.108	0.906	0.871
Equation (2)	0.8	−11.2	0.738	0.637	0.135	0.091	1.095	1.093	0.877	0.837
Equation (2)	0.6	−12.4	0.737	0.651	0.139	0.094	1.106	1.116	0.896	0.863
Equation (2)	0.8	−12.4	0.738	0.636	0.134	0.090	1.099	1.096	0.868	0.828
Equation (2)	0.6	−10.0	0.738	0.653	0.142	0.096	1.098	1.104	0.915	0.880
Equation (2)	0.8	−10.0	0.739	0.638	0.137	0.092	1.091	1.089	0.886	0.845
Mean (‰)			0.730	0.637	0.136	0.092	1.089	1.090	0.882	0.845
Error (‰)			0.009	0.016	0.006	0.004	0.017	0.022	0.033	0.035
Error (%)			1.190	2.504	4.105	4.441	1.527	2.001	3.781	4.098

[a]Spatial $\delta^{18}O_{snow} - T_{sfc}$ equations from *Masson-Delmotte et al.* [2008] (equation (3)) and *Giovinetto and Zwally* [1997] (equation (2)) were used. The temporal relation was taken from *Lhomme* [2004] (equation (4)), in which α_c and β_δ were varied. In these experiments, pCO_2 levels were fixed to 280, 590, 640, and 700 ppm.

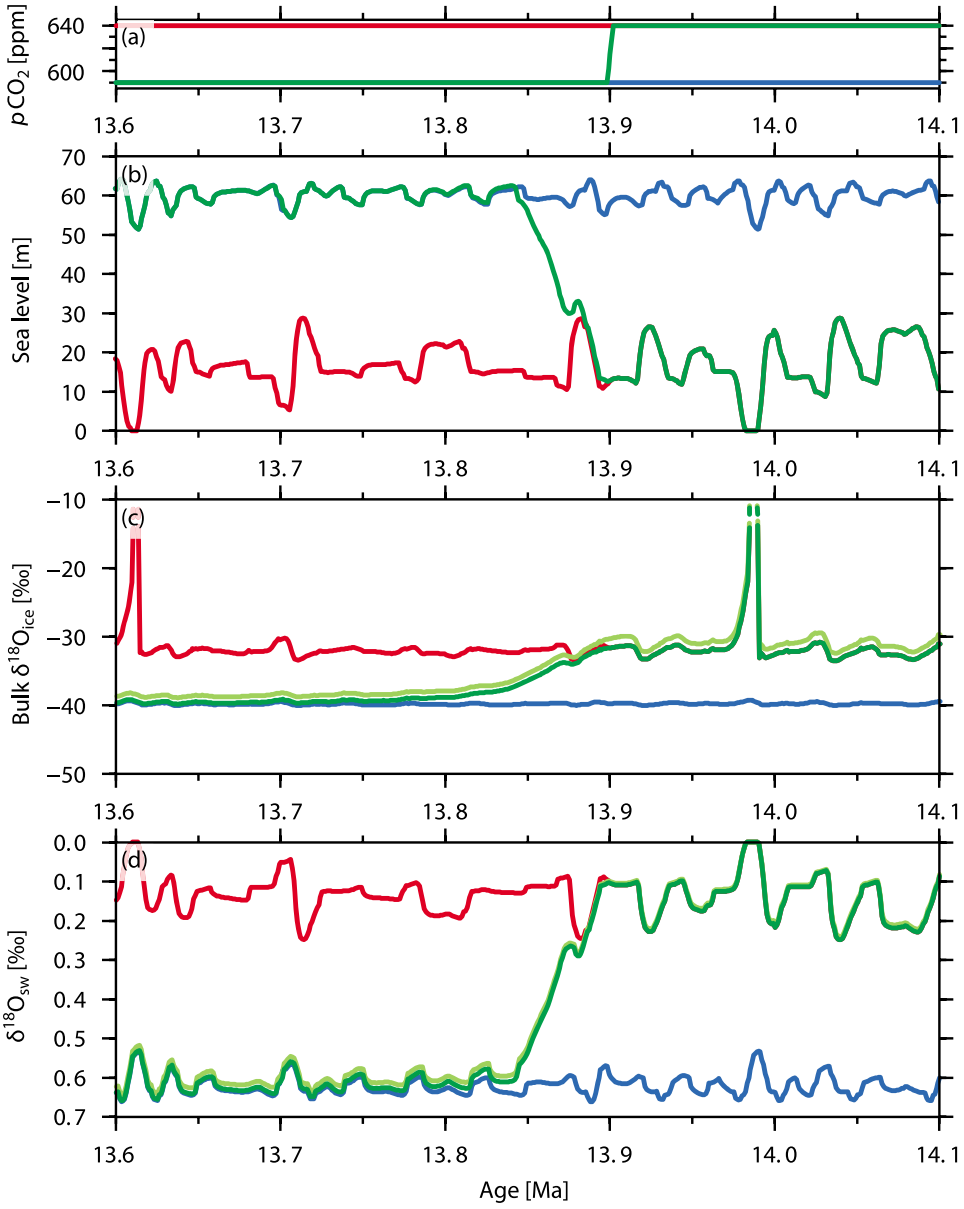

Figure 5. Modeled middle Miocene transition. (a) pCO_2 (ppm), (b) ice volume in sea level equivalents (m), (c) bulk $\delta^{18}O_{ice}$ (‰) and (d) $\delta^{18}O_{sw}$ (‰). Constant pCO_2 forcing of 640 (590) ppm in red (blue). Transient pCO_2 forcing in dark green for α_c = 0.6‰/°C and in light green for α_c = 0.8‰/°C.

transport by changes in the large-scale sea surface temperature distribution and its associated evaporation patterns. This could change the $\delta^{18}O_{snow}$ and the amount of snow, and would therefore alter the mean $\delta^{18}O_{ice}$ of the ice sheet. Unfortunately it is not clear yet to what extent circulation patters were different in the middle Miocene. However, the Antarctic ice sheet was already located at its isolated position at the South Pole, suggesting only minor changes in heat and vapor transport to Antarctica between the middle Miocene and present day. For the long-term experiments in this study, we therefore chose to assume present-day relations between the parameters.

4.2. Sea Level Versus $\delta^{18}O_{sw}$

[31] When no independent information on sea level is available, the part of the measured $\delta^{18}O_c$ which is caused by fluctuations in continental ice volume ($\delta^{18}O_{sw}$) is computed by assuming a linear relation between ice and sea level. From investigating corals, *Fairbanks and Matthews* [1978] derived a value of 1.1‰ $\delta^{18}O_{sw}$ increase for a sea level fall of 100 m. Later studies, using pore fluid to constrain the $\delta^{18}O_{sw}$ of the LGM ocean, resulted in values closer to ~0.8‰/100 m [cf. *Schrag et al.*, 1996; *Adkins and Schrag*, 2001]. Other assessments, combining sea level estimates from backstripping of Oligocene sections with benthic $\delta^{18}O_c$

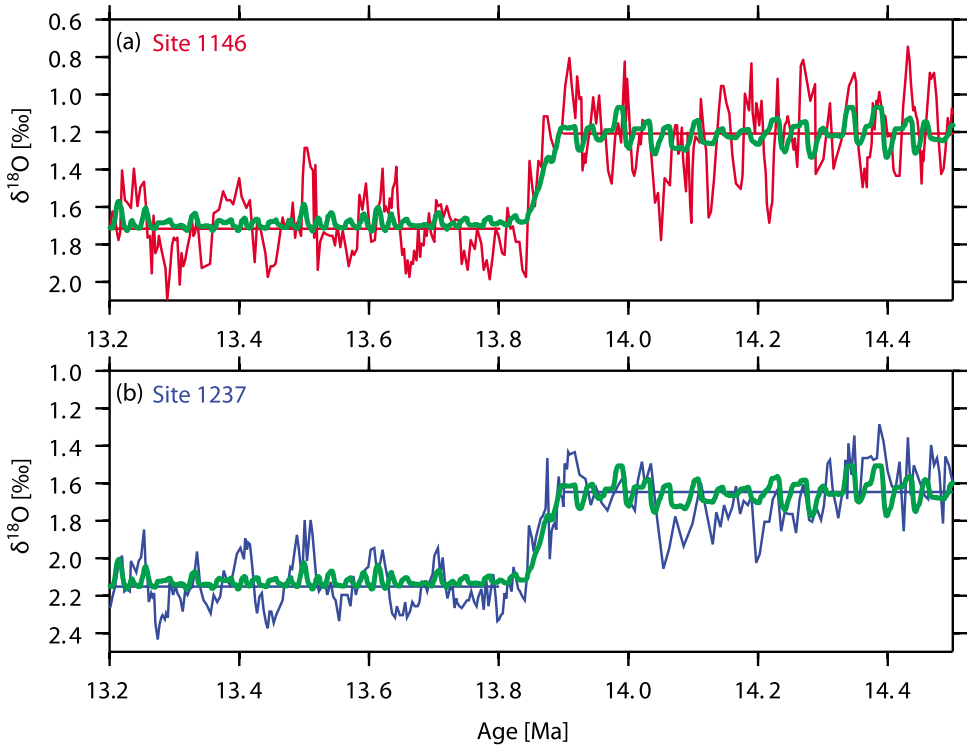

Figure 6. Comparison of modeled $\delta^{18}O_{sw}$ (green) to $\delta^{18}O_c$ from sediment cores. (a) Site 1146 (red) and (b) Site 1237 (blue). For clarity, the model results are shifted to the mean of each proxy record over the period before the transition (13.9–14.5 Ma).

showed a much higher ratio, up to 2.2‰/100 m [*Pekar et al.*, 2002; *Pekar and DeConto*, 2006].

[32] Our simulations forced with a set of different constant pCO_2 levels revealed a mean relation of ~1‰/100 m, thereby confirming the early studies [e.g., *Fairbanks and Matthews*, 1978; *Schrag et al.*, 1996; *Adkins and Schrag*, 2001]. Interestingly, there is a different behavior for the small and the large ice sheets. The $\delta^{18}O_{sw}$ is relatively stronger affected by large ice volumes (~1.08‰/100 m) than by small ice sheets (~0.87‰/100 m).

[33] Both phenomena, the relatively constant relationship between $\delta^{18}O_{sw}$ and S_i and the fact that this ratio slightly varies for differently sized ice sheets, can be explained by equation (5). Taking the derivative of this equation and neglecting a term that is in the order of 10^{-5} yields

$$\frac{\partial \delta^{18}O_{sw}}{\partial S_i} = -\frac{\delta^{18}O_{ice}}{d_0 - S_i}.$$

Typical values for a small ($\delta^{18}O_{ice}$ ~−30‰) and a large ($\delta^{18}O_{ice}$ ~−40‰) ice sheet result in an ~0.8 and 1.1‰ increase of $\delta^{18}O_{sw}$ for a sea level lowering of 100 m. Fixing the mean isotopic ice volume at a value of −35‰ (as implicitly assumed in many studies) leads to the relation of approximately 1‰/100 m, showing only the ice volume effect on the marine oxygen isotopes. The fact that small and large ice sheets have a different mean isotopic content further enhances the influence they have on $\delta^{18}O_{sw}$ or $\delta^{18}O_c$. Small ice sheets have an even smaller imprint on $\delta^{18}O_c$ than expected from the general 1‰/100 m relationship, whereas large ice sheet have a slightly larger impact. However, by accounting for only ~10% of the variation this isotopic effect is much smaller than the ice volume effect.

[34] In order to explain a much higher $\delta^{18}O_{sw}$ to sea level relationship, as proposed by *Pekar et al.* [2002], the isotopic composition of the ice sheet needs to be < −80‰, which seems unrealistically low. Part of the 2.2‰ increase must have been due to an decrease in deep-sea temperature (*Pekar et al.* [2002] suggest about 50%), which recently has been confirmed by a ~2.5 °C cooling for the same site [*Lear et al.*, 2008].

4.3. Oxygen Isotope Transition in the Middle Miocene

[35] We applied the ice sheet–climate model, with $\delta^{18}O$ parameterization included, to the middle Miocene Antarctic glaciation event. Although equation (5) is based on an initial ice-free world, it is thought that small ice sheets already existed on Antarctica [*Zachos et al.*, 2008; *DeConto et al.*, 2008]. We therefore simulated a volume expansion from a small to a large ice sheet. The resulting increase in $\delta^{18}O_{sw}$ is a difference between two states and therefore independent of the assumed initially ice-free conditions of equation (5). *DeConto et al.* [2008] also suggest episodic ice in the Northern Hemisphere. As long as there are no solid constraints on the volume of this ice, it is impossible to consider its effect on global $\delta^{18}O_{sw}$ and we therefore assume that the

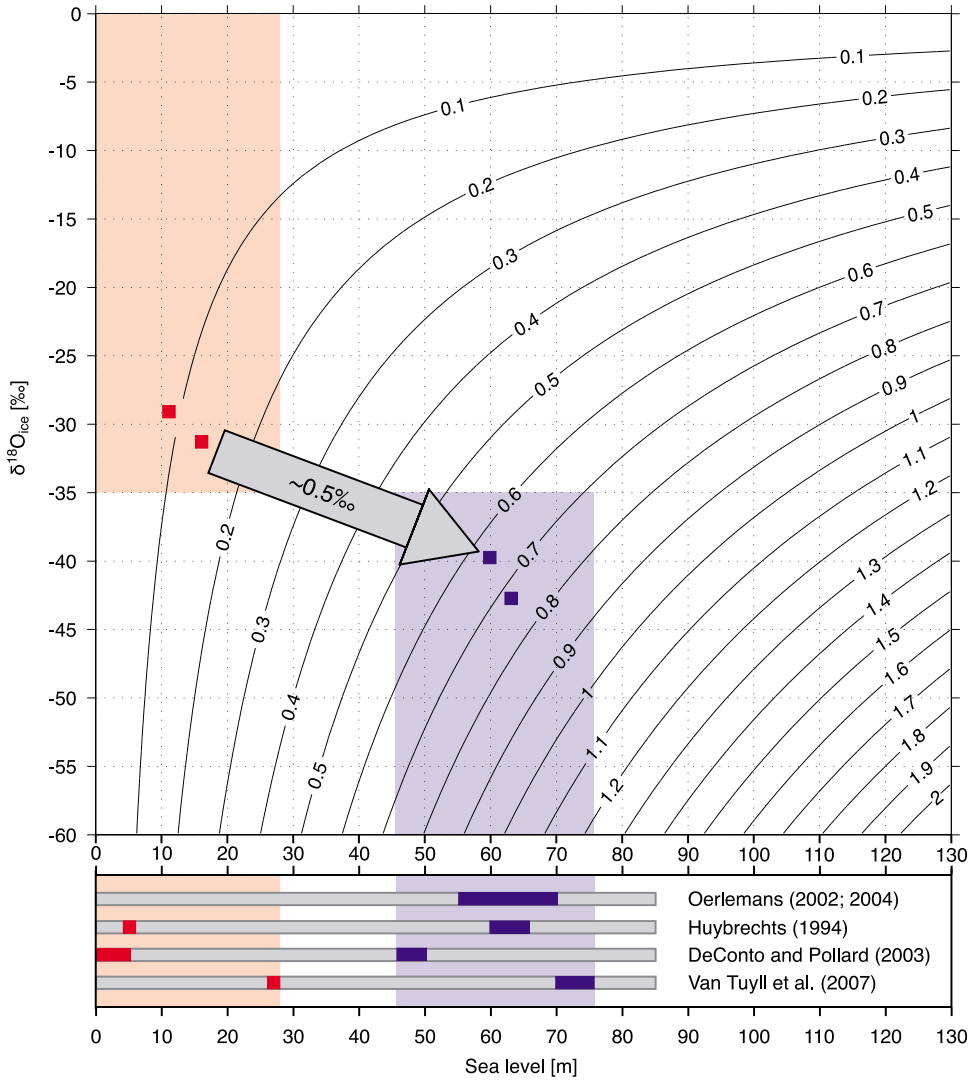

Figure 7. Relationship between sea level (equivalent to ice volume), $\delta^{18}O_{ice}$ and $\delta^{18}O_{sw}$. Contour lines show the resulting $\delta^{18}O_{sw}$ of a combination of sea level–equivalent ice volume and $\delta^{18}O_{ice}$. Estimates for a large present-day or middle Miocene ice sheet vary between 45 and 75 m and small ice sheets range from 2 to 27 m [cf. *Huybrechts*, 1994; *Oerlemans*, 2002; *DeConto and Pollard*, 2003; *Oerlemans*, 2004; *van Tuyll et al.*, 2007] (red and blue colored bars at bottom). The blue and red shaded areas indicate our best guess conditions for a large and a small ice sheet, respectively. Our reference model experiments are shown as red (700 and 640 ppm) and blue (590 and 280 ppm) squares. The arrow indicates the ~0.5‰ $\delta^{18}O_{sw}$ enrichment resulting from the transition from a small to a large ice sheet.

increase in isotopic composition of seawater is only due to ice expansion on Antarctica.

[36] The available high-resolution records of $\delta^{18}O_c$ measured in benthic foraminifera all show a similar trend in the middle Miocene. Between ~13.9 and ~13.8 Ma the mean value increased by approximately 0.5‰ (Table 1 and Figure 1). Our model experiments show a total increase of (0.50 ± 0.02)‰ in $\delta^{18}O_{sw}$, indicating that the mean rise of $\delta^{18}O$ found in the foraminifera could entirely be explained by an increase in ice volume.

[37] In order to assess the effect of a given ice volume change on $\delta^{18}O_{sw}$, we analyze a range of possible scenarios in terms of sea level equivalents and mean isotopic composition of small and large ice sheets (Figure 7). Our modeled ice volume increase leads to an $\delta^{18}O_{sw}$ enrichment of ~0.5‰ (arrow in Figure 7). Taking our best guess for sea level equivalent and $\delta^{18}O_{ice}$ into account (shaded boxes in Figure 7), the smallest $\Delta\delta^{18}O_{sw}$ that can result is ~0.2‰. This estimate is rather insensitive to the exact choice of the $\delta^{18}O_{ice}$ of the small ice sheet, because the $\delta^{18}O_{sw}$ isolines steepen toward low sea level equivalents. *Lhomme et al.* [2005] computed a much more depleted isotopic composition of the present-day East Antarctic ice sheet (~−57‰) than resulted from our model (~−40 to −44‰). However, even if our model overestimates the mean isotopic composition and one assumes that such a bias would also exist for

the middle Miocene ice, the resulting difference in $\delta^{18}O_{sw}$ would be similar.

[38] The middle Miocene increase in ice volume can also be independently deducted from sea level studies, which indicate a sea level drop of 30–40 m [*Miller et al.*, 2005] or 20 ± 15 m [*Kominz et al.*, 2008].

[39] Our experiments suggest a middle Miocene ice sheet expansion in line with these independent sea level estimates and with previous ice volume approximations for large and small ice sheets [e.g., *Huybrechts*, 1994; *Oerlemans*, 2002; *DeConto and Pollard*, 2003; *Oerlemans*, 2004; *van Tuyll et al.*, 2007] (Figure 7). Hence, the modeled increase in $\delta^{18}O_{sw}$ can explain the total mean rise in benthic $\delta^{18}O$ in the middle Miocene.

[40] The individual records, however, show a much larger increase in $\delta^{18}O_c$ when considering the extremes in the record and not the long-term mean values (Figure 1). This remaining increase could well be caused by deep-sea cooling. *Shevenell et al.* [2004, 2008] propose a cooling trend and an Antarctic expansion starting as early as ~15 Ma. From their low-resolution Mg/Ca record they derived a deep-sea cooling of 6 to 7 °C.

[41] The overall much larger variations in the reconstructed $\delta^{18}O_c$ records could reflect the effect of fluctuations in (deep) ocean temperature and salinity. The small temperature variations computed in the lower- and middle-latitude boxes of the ice sheet–climate model are probably too small to explain the large deviations. These temperatures are atmospheric annual mean values for a region of 30° latitude and should show much less variation than local temperature fluctuations of seawater surrounding the foraminifera of a specific deep-sea sediment core. Furthermore, the model forcing was kept (unrealistically) constant at two levels of pCO_2 (590 and 640 ppm). Variations in pCO_2 would also enhance deviations in the modeled $\delta^{18}O_{sw}$ record.

[42] The chosen model parameters or initial conditions could also affect the modeled increase in $\delta^{18}O_{sw}$. For example, another initial bedrock topography would result in different ice volumes, which in turn could change the $\delta^{18}O_{sw}$ values. However, a bedrock or parameter sensitivity study is beyond the scope of this research. Also, we have shown that slight changes in the ice volume and/or $\delta^{18}O_{ice}$ will still result in an increase in $\delta^{18}O_{sw}$ and can largely explain the marine records.

5. Conclusions

[43] According to our model results, we find the following:

[44] 1. The commonly used relation between sea level and $\delta^{18}O_{sw}$ (~1‰/100 m) is also valid for the middle Miocene, because it is determined by the mean depth of the ocean and the mean isotopic composition of the ice sheets of around −35‰.

[45] 2. Large ice sheets are more depleted in heavy oxygen isotopes (~−40‰) and therefore have a relatively large contribution to the isotopic composition of the ocean (~1.08‰ per 100 m). On the other hand, small ice sheets have a relatively small effect with ~0.87‰ per 100 m, due to their less depleted mean isotopic composition (~−30‰). As a result, the assumption of a constant $\delta^{18}O_{ice}$ in ice sheets causes an underestimation of 10% in computed $\delta^{18}O_{sw}$.

[46] 3. An ice volume increase of approximately 15–18 × 10^{15} m^3 (or ~40–50 m sea level equivalent) could explain the mean middle Miocene $\delta^{18}O_c$ shift found in the benthic foraminifera from high-resolution sediment records. About 85% of this was induced by an increase in ice volume and approximately 15% by a stronger depletion of oxygen isotopes in the ice. The remaining part of the transition depicted by the extremes in the $\delta^{18}O_c$ records was probably caused by deep-sea cooling.

[47] **Acknowledgments.** This project was funded by the DFG (Deutsche Forschungsgemeinschaft) within the European Graduate College "Proxies in Earth History." We thank the two anonymous reviewers and D. M. Roche for their constructive comments.

References

Adkins, J. F., and D. P. Schrag (2001), Pore fluid constraints on deep ocean temperature and salinity during the last glacial maximum, *Geophys. Res. Lett.*, *28*, 771–774.

Arthern, R. J., D. P. Winebrenner, and D. G. Vaughan (2006), Antarctic snow accumulation mapped using polarization of 4.3-cm wavelength microwave emission, *J. Geophys. Res.*, *111*, D06107, doi:10.1029/2004JD005667.

Berger, A. L. (1978a), Long term variations of caloric insolation resulting from the Earth's orbital elements, *Quat. Res.*, *9*, 139–167.

Berger, A. L. (1978b), Long term variations of daily insolation and Quaternary climatic changes, *J. Atmos. Sci.*, *35*(12), 2362–2367.

Cuffey, K. M. (2000), Methodology for use of isotope forcings in ice sheet models, *Geophys. Res. Lett.*, *27*, 3065–3068.

Cuffey, K. M., G. D. Clow, R. B. Alley, M. Stuiver, E. Waddington, and R. Saltus (1995), Large Arctic temperature change at the Wisconsin-Holocene glacial transition, *Science*, *270*, 455–458.

DeConto, R. M., and D. Pollard (2003), Rapid Cenozoic glaciation of Antarctica induced by declining atmospheric CO_2, *Nature*, *42*, 245–249.

DeConto, R., D. Pollard, P. A. Wilson, H. Pälike, C. H. Lear, and M. Pagani (2008), Thresholds for Cenozoic bipolar glaciation, *Nature*, *455*, 652–657.

Delaygue, G., J. Jouzel, V. Masson, R. D. Koster, and E. Bard (2000), Validity of the isotopic thermometer in central Antarctica: Limited impact of glacial precipitation seasonality and moisture origin, *Geophys. Res. Lett.*, *27*, 2677–2680.

EPICA Community Members (2004), Eight glacial cycles from an Antarctic ice core, *Nature*, *429*, 623–628.

Fairbanks, R. G., and R. K. Matthews (1978), The marine oxygen isotope record in Pleistocene coral, Barbados, West Indies, *Quat. Res.*, *10*, 181–196.

Giovinetto, M. B., and H. J. Zwally (1997), Areal distribution of the oxygen-isotope ratio in Antarctica: An assessment based on multivariate models, *Ann. Glaciol.*, *25*, 153–158.

Glen, J. W. (1955), The creep of polycrystalline ice, *Proc. R. Soc. London, Ser. A*, *228*, 519–538.

Gonfiantini, R. (1978), Standards for stable isotope measurements in natural compounds, *Nature*, *271*, 534–536.

Helsen, M. M., R. S. W. van de Wal, and M. R. van den Broeke (2007), The isotopic composition of present-day Antarctic snow in a Lagrangian atmospheric simulation, *J. Clim.*, *20*, 739–756.

Holbourn, A., W. Kuhnt, M. Schulz, and H. Erlenkeuser (2005), Impacts of orbital forcing and atmospheric carbon dioxide on Miocene ice-sheet expansion, *Nature*, *438*, 483–487.

Holbourn, A., W. Kuhnt, M. Schulz, J.-A. Flores, and N. Anderson (2007), Orbitally-paced climate evolution during the middle Miocene 'Monterey' carbon-isotope excursion, *Earth Planet. Sci. Lett.*, *261*, 534–550.

Huybrechts, P. (1994), Formation and disintegration of the Antarctic ice sheet, *Ann. Glaciol.*, *20*, 336–340.

Huybrechts, P., D. Steinhage, F. Wilhems, and J. Bamber (2000), Balance velocities and measured properties of the Antarctic ice sheet from a new compilation of gridded data for modeling, *Ann. Glaciol.*, *30*, 52–60.

Intergovernmental Panel of Climate Change (2007), *Climate Change 2007: The Scientific Basis. Contribution of Working Group 1 to the Fourth Assessment Report of the Intergovernmental Panel on Climate Change*, edited by S. Solomon et al., p. 996, Cambridge Univ. Press, Cambridge, U. K.

Jouzel, J., et al. (2007), Orbital and millennial Antarctic climate variability over the past 800,000 years, *Science*, *317*, 793–796.

Kominz, M. A., J. V. Browning, K. G. Miller, P. J. Sugarman, S. Mizintsevaw, and C. R. Scotese (2008), Late Cretaceous to Miocene sea-level estimates from the New Jersey and Delaware coastal plain coreholes: An error analysis, *Basin Res.*, *20*, 211–226.

Langebroek, P. M., A. Paul, and M. Schulz (2009), Antarctic ice-sheet response to atmospheric CO_2 and insolation in the Middle Miocene, *Clim. Past*, *5*, 633–646.

Laskar, J., P. Robutel, F. Joutel, M. Gastineau, A. C. M. Correia, and B. Levrard (2004), A long-term numerical solution for the insolation quantities of the Earth, *Astron. Astrophys.*, *428*, 261–285.

Lear, C. H., H. Elderfield, and P. A. Wilson (2000), Cenozoic deep-sea temperatures and global ice volumes from Mg/Ca in benthic foraminiferal calcite, *Science*, *287*, 269–272.

Lear, C. H., T. R. Bailey, P. N. Pearson, H. K. Coxall, and Y. Rosenthal (2008), Cooling and ice growth across the Eocene-Oligocene transition, *Geology*, *36*, 251–254.

Lhomme, N. (2004), Modelling water istopes in polar ice sheets, Ph.D. thesis, Univ. of British Columbia, Vancouver, B. C., Canada.

Lhomme, N., G. K. C. Clarke, and C. Ritz (2005), Global budget of water isotopes inferred from polar ice sheets, *Geophys. Res. Lett.*, *32*, L20502, doi:10.1029/2005GL023774.

Lisiecki, L. E., and M. E. Raymo (2005), A Pliocene-Pleistocene stack of 57 globally distributed benthic $\delta^{18}O$ records, *Paleoceanography*, *20*, PA1003, doi:10.1029/2004PA001071.

Lythe, M. B., D. G. Vaughan, and the BEDMAP Consortium (2000), BEDMAP—Bed topography of the Antarctic, map, scale 1:10,000,000, Br. Antarct. Surv., Cambridge, United Kingdom.

Masson-Delmotte, V., et al. (2008), A review of Antarctic surface snow isotopic composition: Observations, atmospheric circulation, and isotopic modeling, *J. Clim.*, *21*, 3359–3387.

Miller, K. G., G. S. Mountain, J. V. Browning, M. Kominz, P. J. Sugarman, N. C. Christie-Blick, M. E. Katz, and J. D. Wright (1998), Cenozoic global sea level, sequences, and the New Jersey transect: Results from coastal plain and continental slope drilling, *Rev. Geophys.*, *36*, 569–601.

Miller, K. G., et al. (2005), The Phanerozoic record of global sea-level change, *Science*, *310*, 1293–1298.

Mix, A. C., and W. F. Ruddiman (1984), Oxygen-isotope analysis and Pleistocene ice volumes, *Quat. Res.*, *21*, 1–20.

Oerlemans, J. (2002), Global dynamics of the Antarctic ice sheet, *Clim. Dynam.*, *19*, 85–93.

Oerlemans, J. (2004), Antarctic ice volume and deep-sea temperature during the last 50 Myr: A model study, *Ann. Glaciol.*, *309*, 600–603.

Payne, A. J., and P. W. Dongelmans (1997), Self-organization on the thermomechanical flow of ice sheets, *J. Geophys. Res.*, *106*, 12,219–12,233.

Pekar, S. F., and R. M. DeConto (2006), High-resolution ice-volume estimates for the early Miocene: Evidence for a dynamic ice sheet in Antartica, *Palaeogeogr. Palaeoclimatol. Palaeoecol.*, *231*, 101–109.

Pekar, S. F., N. Christie-Blick, M. A. Kominz, and K. G. Miller (2002), Atmospheric carbon dioxide concentrations over the past 60 million years, *Geology*, *30*, 903–906.

Pollard, D. (1982), A simple ice sheet model yields realistic 100 kyr glacial cycles, *Nature*, *296*, 334–338.

Raffi, I., J. Backman, E. Fornaciari, H. Pälike, D. Rio, L. Lourens, and F. Hilgen (2006), A review of calcareous nannofossil astrobiochronology encompassing the past 25 million years, *Quat. Sci. Rev.*, *25*, 3113–3137.

Schrag, D. P., G. Hampt, and D. W. Murray (1996), Pore fluid constraints on the temperature and oxygen isotopic composition of the Glacial Ocean, *Science*, *272*, 1930–1932.

Shackleton, N. J. (1974), Attainment of isotopic equilibrium between ocean water and the benthoic foraminifera genus Unigerina: Isotopic changes in the ocean during the last glacial, *Cent. Natl. Sci. Colloq. Int.*, *219*, 203–209.

Shevenell, A. E., and J. P. Kennett (2004), Paleoceanographic change during the Middle Miocene climate revolution: An Antarctic stable isotope perspective, in *The Cenozoic Southern Ocean: Tectonics, Sedimentation and Climate Change Between Australia and Antarctica*, *Geophys. Monogr. Ser.*, vol. 151, edited by N. Exon, J. Kennett, and M. Malone, AGU, Washington, D. C.

Shevenell, A., J. P. Kenneth, and D. W. Lea (2004), Middle Miocene Southern Ocean cooling and Antarctic cryosphere expansion, *Science*, *305*, 1766–1770.

Shevenell, A., J. P. Kenneth, and D. W. Lea (2008), Middle Miocene ice sheet dynamics, deep-sea temperatures, and carbon cycling: A Southern Ocean perspective, *Geochem. Geophys. Geosyst.*, *9*, Q02006, doi:10.1029/2007GC001736.

Sima, A. (2005), Modeling oxygen isotopes in ice sheets linked to Quaternary ice-volume variations, Ph.D. thesis, Univ. of Bremen, Bremen, Germany.

Sima, A., A. Paul, M. Schulz, and J. Oerlemans (2006), Modeling the oxygen-isotopic composition of the North American Ice Sheet and its effect on the isotopic composition of the ocean during the last glacial cycle, *Geophys. Res. Lett.*, *33*, L15706, doi:10.1029/2006GL026923.

van de Berg, W. J., M. R. van den Broeke, C. H. Reijmer, and E. van Meijgaard (2006), Reassessment of the Antarctic surface mass balance using calibrated output of a regional atmospheric climate model, *J. Geophys. Res.*, *111*, D11104, doi:10.1029/2005JD006495.

van Tuyll, C. I., R. S. W. van de Wal, and J. Oerlemans (2007), The response of a simple Antarctic ice flow model to temperature and sea level fluctuations over the Cenozoic era, *Ann. Glaciol.*, *46*, 69–77.

Waelbroeck, C., L. Labeyrie, E. Michel, J. C. Duplessy, J. F. McManus, K. Lambeck, E. Balbon, and M. Labracherie (2002), Sea-level and deep water temperature changes derived from benthic foraminifera isotopic records, *Quat. Sci. Rev.*, *21*, 295–305.

Zachos, J. C., M. Pagani, L. Sloan, E. Thomas, and K. Billups (2001), Trends, rhythms, and aberrations in global climate 65 Ma to present, *Science*, *292*, 686–693.

Zachos, J. C., G. R. Dickens, and R. E. Zeebe (2008), An early Cenozoic perspective on greenhouse warming and carbon-cycle dynamics, *Nature*, *451*, 279–283.

Zwally, H. J., M. Giovinetto, M. Craveb, V. Morgan, and I. Goodwin (1998), Areal distribution of the oxygen-isotope ration in Antarctica: Comparison of results based on field and remotely sensed data, *Ann. Glaciol.*, *27*, 583–590.

P. M. Langebroek, Alfred Wegener Institute for Polar and Marine Research, D-27570 Bremerhaven, Germany. (petra.langebroek@awi.de)

A. Paul and M. Schulz, Faculty of Geosciences, University of Bremen, Postbox 330440, D-28334 Bremen, Germany.